a clear oil: 160 mg, 32%; ^{1}H NMR δ 0.92 (t, 3 H, J = 6.9), 1.06 (d, 3 H, J = 6.6), 1.4 (m, 2 H), 1.55 (m, 4 H), 3.15 (m, 1 H), 3.23 (m, 1 H), 4.56 (m, 2 H), 7.3 (m, 5 H).

Determination of Optical Purity. Each amino ether was N-acylated with either *N*-(phenylsulfonyl)prolyl chloride[12] or mandelic acid-isobutylcarbonic acid anhydride. When racemic N-acylating agents were used, the resulting diastereomeric amides were shown to be separable and of equal concentration by analytical HPLC. When optically pure N-acylating agents were used, HPLC showed that >99% (the limit of detection) of one diastereomer was present. The *N*-(phenylsulfonyl)-proline derivatives were chromatographed on a normal phase column, eluting with CH_2Cl_2/isopropyl alcohol, 99.75/0.25. The mandelic acid derivatives were chromatographed on a reverse phase column, eluting with H_2O/CH_3CN, 75/25, 65/35, or 45/55.

Preparation of Mandelic Acid Amides. L- or D,L-mandelic acid (0.68 mmol, 103 mg) was dissolved in THF (4 mL), cooled to -15 °C, and treated with *N*-methylmorpholine (0.68 mmol, 75 μL) followed by isobutyl chloroformate (0.62 mmol, 80 μL). The resulting solution was stirred for 60 s and then a precooled solution of amino ether (0.22 mmol) in THF (1 mL) was added. The solution was stirred an additional 45 min at -15 °C. Solvent was evaporated, and the residue was partitioned between 10% aqueous citric acid (10 mL) and EtOAc (10 mL). The aqueous layer was reextracted with EtOAc (2 × 10 mL), and the combined organic layer was washed with saturated $NaHCO_3$ (2 × 10 mL) and brine (10 mL), dried, and evaporated. The residue contains the isobutyl carbonate of the mandelic amide which is suitable for HPLC analysis. More sensitive analyses result from the mandelic amide, obtained by dissolving the carbonate in MeOH (5 mL) and treating with pH 8 phosphate buffer (5 mL) for 17 h.

Configurational Stability Studies of *N*-(9-(9-Phenylfluorenyl))-L-alaninal (5). Solutions of 0.1 M *N*-(PhFl)-L-alaninal (**5**) in THF alone or in the presence of 100 mol % of triethylamine or 100 wt % silica gel were stirred for 24 h at room temperature or 1 h at reflux and then evaporated. The optical rotations of the remaining solids showed no decrease in rotation. An analogous solution of **5** and triethylamine in THF was heated at reflux 8 h, and an aliquot was concentrated to an oil which was chromatographed (Chromatotron), eluting with 10% EtOAc in hexane. Eluting first was 9-phenylfluorene followed by aldehyde **5** which showed no loss in optical rotation. The remaining solution was chilled to 0 °C, treated with excess $NaBH_4$, stirred 1 h, and poured into 1 M NaH_2PO_4. The aqueous layer was extracted with EtOAc, and the combined organic layer was washed with brine, dried, filtered, and evaporated to an oil which was chromatographed on silica gel, eluting with hexane/EtOAc, 2/1. Concentration of the collected fractions gave **6** which was subsequently converted to its mandelic amide and shown to be >99% enantiomerically pure by HPLC analysis.

Simple General Acid-Base Catalysis and Virtual Transition States for Acetylcholinesterase-Catalyzed Hydrolysis of Phenyl Esters

Scott A. Acheson, Dimitra Dedopoulou, and Daniel M. Quinn*

Contribution from the Department of Chemistry, University of Iowa, Iowa City, Iowa 52242.
Received December 27, 1985

Abstract: Acetylcholinesterase-catalyzed hydrolyses of the acetyl esters phenyl acetate and *o*-nitrophenyl acetate and of the chloroacetyl esters phenyl chloroacetate and *p*-methoxyphenyl chloroacetate have been investigated. V's are quantitatively similar for the constituents of each pair of esters, which indicates that deacylation is partly rate limiting when the enzyme is saturated by substrate. Solvent deuterium isotope effects for V/K are near unity, which is consistent with virtual acylation transition states that are prominently rate limited by nonchemical events [Quinn, D. M.; Swanson, M. L. *J. Am. Chem. Soc.* **1984**, *106*, 1883-1884]. On the other hand, solvent deuterium isotope effects for V fall in the range 1.6-2.26 and are interpreted in terms of transition states that are stabilized by solvation catalytic proton bridges. The Eyring plot constructed from initial velocities of AChE-catalyzed hydrolysis of *o*-nitrophenyl acetate at $[S]_0 \gg K$ is nonlinear downward and is interpreted in terms of prominent rate determination from both acylation and deacylation. However, the solvent isotope effect for the reaction is independent of temperature, which indicates that the solvent isotope effects for the acylation and deacylation components of V must be of comparable magnitude. Proton inventory plots of partial solvent isotope effects on initial velocities at $[S]_0 \gg K$ vs. the atom fraction of deuterium in mixed H_2O-D_2O buffers are linear for the substrates phenyl chloroacetate and *o*-nitrophenyl acetate. Therefore, AChE behaves as a simple general acid-base catalyst for the studied ester hydrolyses. pL-rate profiles (L = H, D) for hydrolysis of *o*-nitrophenyl acetate are sigmoidal in shape, and nonlinear-least-squares analysis gives $pK_a^{H_2O} = 6.31 \pm 0.03$, $pK_a^{D_2O} = 6.81 \pm 0.03$, and $^{D_2O}V_{i,lim} = 1.82 \pm 0.02$. The β-deuterium secondary isotope effect for *o*-nitrophenyl acetate hydrolysis is $^{D3}V_i = 0.96_0 \pm 0.01_7$. These results are interpreted in terms of a virtual transition state for AChE-catalyzed ester hydrolysis that is a weighted average of acylation and deacylation transition states that are each stabilized by single-proton transfers.

The broad strokes of acetylcholinesterase (AChE[1]) catalysis have been appreciated for some years.[2,3] The AChE mechansim involves nucleophilic serine and general acid-base[3,4] catalytic elements and an acylenzyme intermediate, as outlined in Scheme I, where Im represents the imidazole side chain of the active site histidine. The mechanism of Scheme I is analogous to that of the serine proteases.[5,6] The details of AChE catalysis are not well-defined, however. Rosenberry has measured kinetic solvent deuterium isotope effects of 2-3 for V of AChE-catalyzed hydrolysis of acetate esters.[3,4] Do isotope effects of this magnitude arise because the enzyme stabilizes chemical transition states via single-proton bridges (as Scheme I implies) or via concerted proton transfers (as in the case of serine protease catalyzed hydrolysis of peptide substrates[7-11])? Are proton transfers and nucleophilic

Scheme I

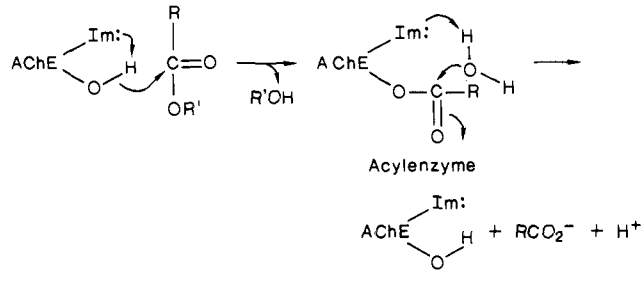

* Author to whom correspondence should be addressed.

0002-7863/87/1509-0239$01.50/0

enzyme–substrate interactions occurring simultaneously, as Scheme I shows? We address these questions in this manuscript by using two pairs of acyl-similar AChE substrates, the acetate esters *o*-nitrophenyl acetate (ONPA) and phenyl acetate (PA) and the chloroacetate esters phenyl chloroacetate (PCA) and *p*-methoxyphenyl chloroacetate (PMPCA). V for these esters monitors a mix of rate-determining acylation and deacylation, whereas V/K always monitors rate-determining acylation. Therefore, information on the molecular dynamics of both the acylation and deacylation stages of AChE catalysis is obtained.

Experimental Section

Materials. Inorganic buffer components were reagent grade and were used without further purification. Grade V-S AChE (EC 3.1.1.7) from *Electrophorus electricus* was obtained as a lypholized powder from Sigma. Prior to use the enzyme was dissolved in 0.1 M sodium phosphate buffer, pH 7.30, that contained 0.1 N NaCl. AChE active site concentrations were determined by fluorescent titration with *N*-methyl-7-(dimethylcarbamoxy)quinolinium iodide, as described by Rosenberry and Bernhard.[12] Protium oxide was distilled and deionized. Deuterium oxide (>99.9% D) and acetonitrile (spectrophotometric grade) were obtained from Aldrich and were used as received. ONPA, PA, *o*-nitrophenol, phenol, *p*-methoxyphenol, deuteriated acetic anhydride (>99.9% D), chloroacetic anhydride, and triethylamine were obtained from Sigma. Anhydrous diethyl ether was obtained from Mallinckrodt, silica gel (60–200 mesh) from J. T. Baker, and precoated TLC plates from Machery-Nagel. Phenol was purified by vacuum sublimation, and triethylamine was distilled prior to use.

Substrates. The deuteriated isotopomer of ONPA was prepared and purified according to a published procedure and had a melting point of 37–38 °C [lit. mp 38 °C[13]]. Deuterium incorporation was estimated by NMR to be no less than 97%. PCA was prepared by reaction of chloroacetic anhydride with phenol. One equivalent of chloroacetic anhydride in anhydrous diethyl ether was added to a solution of phenol in ether that contained 1.2 equiv of triethylamine. The mixture was stirred for 24 h at room temperature and washed with 0.1 N hydrochloric acid, 0.1 N sodium bicarbonate, and water. The ether solution was dried over magnesium sulfate, and the ether was evaporated. The crude ester was purified by column chromatography on silica gel with methylene chloride as the eluent. The purified PCA had a melting point of 39–40 °C [lit. mp 40–41 °C[14]]. PMPCA was prepared in a similar fashion and recrystallized twice from aqueous EtOH (mp 44 °C). Each substrate gave a single spot when analyzed by TLC on precoated silica slides with methylene chloride as the eluent for ONPA, PA, and PMPCA and chloroform as the eluent for PCA.

Kinetic Measurements and Data Reduction. Time course data (digital absorbance readings vs. time) were acquired and analyzed by using an IBM personal computer that is interfaced to a Beckman DU-7 UV–vis spectrophotometer. Time courses were followed at 410 nm for ONPA, 270 nm for PA and PCA, and 290 nm for PMPCA. Reactions were conducted in 1.00 mL of solution in a quartz cuvette in the water-jacketed cell holder of the DU-7. Temperature was maintained (±0.05 °C) by a VWR 1140 circulating water bath. The pH values of buffer solutions were measured with a Corning Model 125 pH meter equipped with a glass combination electrode. For deuterium oxide buffers, 0.4 was added to the pH meter reading.[15] Equivalent H_2O and D_2O buffers[16,17] were used for solvent isotope effect measurements and proton inventories. Equivalent buffers are those for which the concentrations of respective components are the same. For a set of equivalent buffers, the pD of the D_2O buffer is greater than the pH of the H_2O buffer by ~0.5 pH unit. This shift is due to a solvent isotope effect on the pK_a of the acid component of the buffer and matches pK_a shifts for a wide range of weak organic acids.[16,17]

Initial velocities were determined by linear-least-squares analysis of time course data that comprised <5% of total substrate turnover. Initial velocities for nonenzymic hydrolysis of PCA and of ONPA at pH ≥7.50 were subtracted from initial velocities for reactions with AChE present. Nonenzymic hydrolysis of PA was negligible under the conditions used. Enzyme kinetic parameters, V and K, were calculated by nonlinear-least-squares fitting of initial rate vs. initial substrate concentration data to the hyperbolic Michaelis–Menten equation (eq 1), where V_i is the

$$V_i = \frac{V[S]_o}{K + [S]_o} \quad (1)$$

initial velocity, $[S]_o$ is the initial substrate concentration, V is the maximal velocity, and K is the Michaelis constant. First-order rate constants (V/K) were measured by using $[S]_o < 0.1K$ and were calculated by nonlinear-least-squares fitting of time course data to the following exponential function:

$$A = (A_o - A_{inf})e^{-(V/K)t} + A_{inf} \quad (2)$$

In eq 2 A is the absorbance at time t, A_o and A_{inf} are the absorbances at $t = 0$ and $t =$ infinite time, respectively, and V/K is the first-order rate constant. First-order reactions were followed for at least three half-lives. The pK_a's that govern V in protium and deuterium oxide were calculated by nonlinear-least-squares fitting of initial rate vs. hydrogen ion or deuterium ion concentration data to eq 3, where V_i is the initial velocity, $[L^+]$ is the hydrogen or deuterium ion concentration, $V_{i,lim}$ is the limiting velocity at high pL, and K_a is the ionization constant for a single titrable amino acid side chain.

$$V_i = \frac{V_{i,lim}K_a}{K_a + [L^+]} \quad (3)$$

Table I. Kinetic Parameters and Solvent Isotope Effects for AChE-Catalyzed Hydrolysis of Phenyl Esters

substrate	$10^{-3}k_{cat}$, s^{-1} [a]	K, mM[a]	^{D_2O}V	$^{D_2O}(V/K)$
ONPA	2.00 ± 0.03	0.26 ± 0.02	1.89 ± 0.06[b]	1.07 ± 0.03[c]
PA	2.72 ± 0.03	1.42 ± 0.05	2.26 ± 0.06[d]	1.33 ± 0.02[c]
				1.16 ± 0.08[d]
PCA	0.37 ± 0.01	0.17 ± 0.05	1.81 ± 0.04[b]	1.0 ± 0.1[e]
PMPCA	0.20 ± 0.02	0.8 ± 0.1	1.6 ± 0.1[f]	0.93 ± 0.02[g]

[a] ONPA and PA reactions were conducted at 25.00 ± 0.05 °C in 0.1 M sodium phosphate buffer, pH 7.30, that contained 0.1 N NaCl, 0.61 nM AChE, and 2% CH_3CN (v/v). PCA and PMPCA reactions were conducted at 20.00 ± 0.05 °C in 0.1 M sodium phosphate buffer, pH 6.08, that contained 0.1 N NaCl, 5.1 nM AChE, and 2% CH_3CN (v/v). K and V were calculated by nonlinear-least-squares fitting of V_i vs. $[S]_0$ data to eq 1. [b] See Figure 2 caption. [c] Reactions were conducted at 25.00 ± 0.05 °C in 0.1 M sodium phosphate buffer, pH 7.30 or pD 7.85, that contained 0.1 N NaCl, 4.8 nM AChE, ($[ONPA]_0$ = 20 μM or $[PA]_0$ = 50 μM), and 2% CH_3CN (v/v). The isotope effect on V/K was calculated from rate constants determined by nonlinear-least-squares fitting of time course data to eq 2. [d] Same conditions as in footnote *a*, except that pD = 7.85 and the reactions contained 1.27 nM AChE. K and V were calculated by fitting V_i vs. $[S]_0$ data to eq 1. [e] Same as footnote *a*, except that pH = 6.12, pD = 6.67, the reactions contained 3.05 nM AChE, and $[PCA]_0$ = 15 μM. The isotope effect for V/K was calculated from rate constants determined by nonlinear-least-squares fitting of time course data to eq 2. [f] Same as footnote *a*, except that pH = 6.11 and pD = 6.67. [g] Same as footnote *e*, except that the reactions contained 5.1 nM AChE and $[PMPCA]_0$ = 50 μM.

(1) Abbreviations: ONPA, *o*-nitrophenyl acetate; PCA, phenyl chloroacetate; PA, phenyl acetate; PMPCA, *p*-methoxyphenyl chloroacetate; AChE, acetylcholinesterase; V, maximal velocity V_{max}; V_i, initial velocity; K, Michaelis constant K_m; ^{D_2O}V, kinetic solvent deuterium isotope effect for V; β-D effect, kinetic β-deuterium secondary isotope effect; ^{D3}V, kinetic β-deuterium secondary isotope effect for V; pL, pH or pD; $[E]_T$, analytical enzyme concentration.

(2) Froede, J. S.; Wilson, I. B. In *The Enzymes*, 3rd ed.; Boyer, P. D., Ed.; Academic: New York, 1971; Vol. 5, pp 87–114.
(3) Rosenberry, T. L. *Adv. Enzymol. Rel. Areas Mol. Biol.* **1975**, *43*, 103–218.
(4) Rosenberry, T. L. *Proc. Natl. Acad. Sci. U.S.A.* **1975**, *72*, 3834–3838.
(5) Blow, D. M. *Acc. Chem. Res.* **1976**, *9*, 145–152.
(6) Stroud, R. M. *Sci. Am.* **1974**, *231*, 74–88.
(7) Hunkapiller, M. W.; Forgac, M. D.; Richards, J. H. *Biochemistry* **1976**, *15*, 5581–5588.
(8) Elrod, J. P.; Hogg, J. L.; Quinn, D. M.; Venkatasubban, K. S.; Schowen, R. L. *J. Am. Chem. Soc.* **1980**, *102*, 3917–3922.
(9) Stein, R. L.; Elrod, J. P.; Schowen, R. L. *J. Am. Chem. Soc.* **1983**, *105*, 2446–2552.
(10) Stein, R. L. *J. Am. Chem. Soc.* **1983**, *105*, 5111–5116.
(11) Stein, R. L. *J. Am. Chem. Soc.* **1985**, *107*, 5767–5775.
(12) Rosenberry, T. L.; Bernhard, S. A. *Biochemistry* **1971**, *10*, 4114–4120.
(13) Galatis, L. G. *J. Am. Chem. Soc.* **1947**, *69*, 2062.
(14) *Sadtler Standard Spectra*; Sadtler Research Laboratories, Inc.: Philadelphia, 1975; Vol. 85, UV spectrum 22737.
(15) Salomaa, P.; Schaleger, L. L.; Long, F. A. *J. Am. Chem. Soc.* **1964**, *86*, 1–7.
(16) Schowen, K. B. J. In *Transition States of Biochemical Processes*; Gandour, R. D., Schowen, R. L., Eds.; Plenum: New York, 1978; pp 225–283.
(17) Schowen, K. B.; Schowen, R. L. *Methods Enzymol.* **1982**, *87*, 551–606.

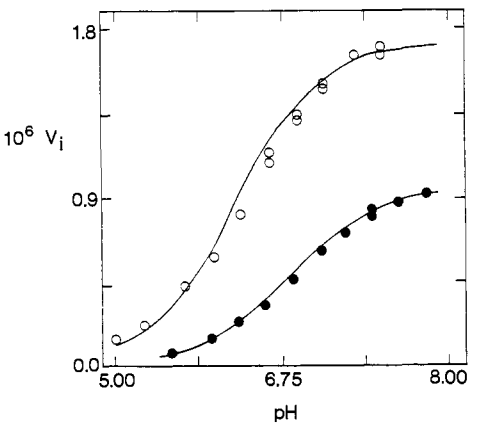

Figure 1. pL–rate profiles (L = H, D) for initial velocities at $[ONPA]_o$ = 2.00 mM. Reactions were conducted at 25.00 ± 0.05 °C at the indicated pH in 1.00 mL of D_2O (closed circles) or H_2O (open circles) that contained 0.1 N NaCl, 0.64 nM AChE, and 2% CH_3CN (v/v). Buffers were 0.1 M sodium phosphate at pH ≥ 5.72 and at pD ≥ 6.28 and 0.1 M sodium citrate otherwise.

Computational methods for analyzing proton inventory data and Eyring plot data are described in the Results section.

Results

Solvent Isotope Effects for V and V/K. Table I lists the enzyme kinetic parameters k_{cat} and K and the solvent deuterium kinetic isotope effects for V and V/K for the four substrates employed in this study. For the sets of esters that have identical acyl groups (i.e., acetyl for ONPA and PA; chloroacetyl for PCA and PMPCA), V's are quantitatively similar. Hence, at substrate saturation either deacylation is the rate-determining step or both acylation and deacylation are contributing to rate determination. The latter interpretation is favored for reasons that will be discussed later. Since k_{cat} is ~10-fold higher for ONPA and PA than for PCA and PMPCA, the physiologically-relevant deacetylation reaction is faster than dechloroacetylation.

pL–Rate Profiles. Figure 1 contains the pL–rate profiles (L = H, D) for V_i for AChE-catalyzed hydrolysis of ONPA. Initial velocities were measured at $[S]_o$ = 2.0 mM as a function of hydrogen ion and deuterium ion concentration. At pH 7.30 and pD 7.85, $[S]_o = 7.7K$ (89% of the maximal velocity, V) and $12K$ (92% of the maximal velocity), respectively. At pH 5.00, K = 0.13 mM, so that $[S]_o = 15K$ and the reaction rate is 94% V. Because the fractional saturation of the enzyme is high (i.e., V_i ~90% V) and does not vary appreciably with pH, the pL–rate profiles of Figure 1 monitor the pL dependences of V. The pK_a of 6.31 ± 0.03 in protium oxide and the pK_a of 6.81 ± 0.03 in deuterium oxide are consistent with dependence of AChE activity on the basic form of an active site histidine amino acid side chain.[2,3]

Proton Inventories. Figure 2 displays the proton inventories for V_i's measured at $[S]_o \gg K$ for AChE-catalyzed hydrolysis of ONPA and PCA. The corresponding data are listed in Table II. The theory and application of the proton inventory technique have been thoroughly described.[16,17] Initial velocities were measured in protium oxide and binary mixtures of protium and deuterium oxide. Polynomial regression analysis[18] for both proton inventories indicated that only the linear terms were significant at the 99.9% confidence level. None of the higher order terms (quadratic through quintic) were significant at the 80% confidence level. These analyses indicate that the proton inventories are best described by linear functions

$$V_{i,n} = V_{i,o}(1 - n + n\Phi^T) \quad (4)$$

where $V_{i,n}$ and $V_{i,o}$ are initial velocities in mixed solvents of atom fraction of deuterium n and in H_2O, respectively; Φ^T is the transition-state fractionation factor. Thus, both reactions involve single-transition-state proton bridges. Linear-least-squares fits to eq 4 give $V_{i,o}$ = 1.44 ± 0.01 × 10^{-6} M s^{-1}, Φ^T = 0.53 ± 0.02 (ONPA); and $V_{i,o}$ = 1.481 ± 0.008 × 10^{-6} M s^{-1}, Φ^T = 0.55 ± 0.01 (PCA). The solvent isotope effects (i.e., the reciprocals of

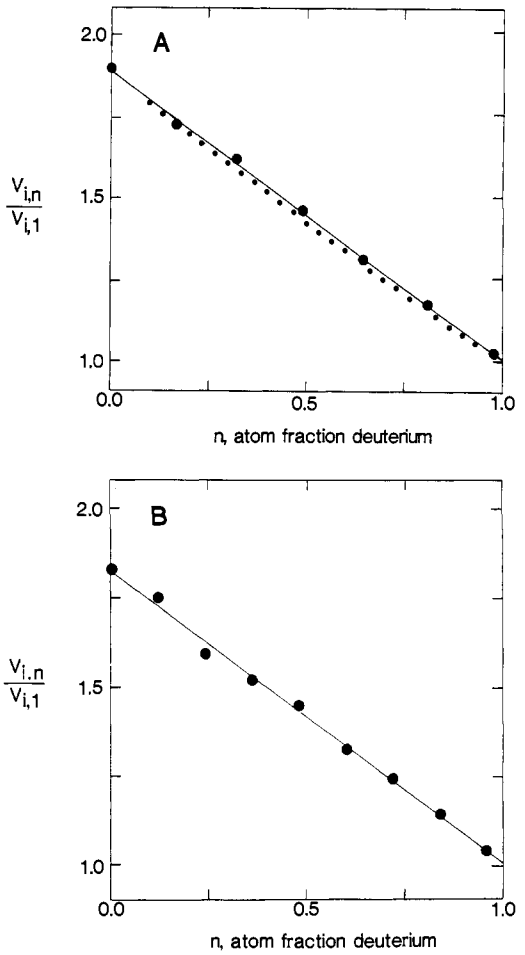

Figure 2. Proton inventories for AChE-catalyzed reactions. The data are plotted as partial solvent isotope effects ($V_{i,n}/V_{i,1}$) vs. n, where $V_{i,1}$ is the extrapolated initial velocity in 100% D_2O calculated from fits to eq 4. (A) Proton inventory plot for AChE-catalyzed hydrolysis of ONPA. Reactions were conducted at 25.00 ± 0.05 °C in 1.00 mL of 0.1 M sodium phosphate buffer, pH 7.30 and equivalent pL,[16,17] that contained 0.1 N NaCl ($[ONPA]_o$ = 2.00 mM), 0.64 nM AChE, and 2% CH_3CN (v/v). (B) Proton inventory plot for AChE-catalyzed hydrolysis of PCA. Reactions were conducted at 20.00 ± 0.05 °C in 1.00 mL of 0.1 M sodium phosphate buffer, pH = 6.12 and equivalent pL,[16,17] that contained 0.1 N NaCl ($[PCA]_o$ = 4.00 mM), 4.1 nM AChE, and 2% CH_3CN (v/v).

Table II. Initial Velocities for AChE-Catalyzed Hydrolysis of ONPA and PCA in Binary Mixtures of H_2O and D_2O[a]

ONPA		PCA	
n	10^6V_i, M s^{-1}	n	10^6V_i, M s^{-1}
0.978	0.771, 0.781	0.957	0.849, 0.834
0.811	0.889, 0.892	0.838	0.921, 0.935
0.644	0.974, 0.994	0.719	1.013, 1.003
	1.023		
		0.599	1.086, 1.059
0.489	1.085, 1.129		
		0.479	1.163, 1.182
0.319	1.205, 1.246		
		0.359	1.252, 1.217
0.165	1.312, 1.313		
		0.241	1.314, 1.272
0.000	1.374, 1.477		
	1.427, 1.482	0.120	1.428, 1.415
		0.000	1.483, 1.483

[a] Refer to the Figure 2 caption for reaction conditions.

(18) *BMDP Statistical Software*; Dixon, W. J., Ed.; University of California Press: Berkeley, 1983; pp 283–304. Polynomial regression analysis is described on pp 283–288. The nonlinear-least-squares computer program, which we used to calculate fits to eq 5, is described on pp 289–304.

Table III. β-Deuterium Secondary Isotope Effects for AChE-Catalyzed Hydrolysis of ONPA

experiment	10^6V_i, M s^{-1} H3[a]	10^6V_i, M s^{-1} D3[a]	^{D3}V
1[b]	1.014		0.973
		1.042	0.959
	0.999		0.938
		1.065	0.940
	1.001		0.978
		1.024	0.987
	1.011		0.982
		1.030	0.966
	0.995		0.951
		1.046	0.966
	1.010		0.944
		1.070	*d*
2[c]	1.503		0.922
		1.631	0.938
	1.530		0.957
		1.598	0.977
	1.562		0.968
		1.614	0.949
	1.531		0.972
		1.575	0.975
	1.535		0.961
		1.597	0.961
	1.535		0.967
		1.587	*e*

[a] H3 and D3 signify the acetyl-H_3 and the acetyl-D_3 isotopomers of ONPA, respectively. [b] Reactions were conducted at 25.00 ± 0.05 °C in 0.1 M sodium phosphate buffer, pH 7.30, that contained 0.1 N NaCl, 0.32 nM AChE ($[ONPA]_0$ = 2.00 mM), and 2% CH_3CN (v/v). [c] Same conditions as footnote *b*, except pH = 7.15 and the reactions contained 0.64 nM of AChE. [d] Mean = $0.96_2 \pm 0.01_7$. [e] Mean = $0.95_9 \pm 0.01_7$.

Φ^T's) are 1.89 ± 0.06 for ONPA and 1.81 ± 0.04 for PCA and are consistent with stabilization of transition states for chemical steps of AChE catalysis by solvation catalytic bridges.[19] As a check on this single-proton-bridge model, the proton inventories were fit to the following quadratic equation, which is predicated on a two-proton model:

$$V_{i,n} = V_{i,o}(1 - n + n\Phi_1^T)(1 - n + n\Phi_2^T) \quad (5)$$

Nonlinear-least-squares fits to eq 5 give $\Phi_1^T = 0.543 \pm 0.007$ and $\Phi_2^T = 0.98 \pm 0.02$ for ONPA, and $\Phi_1^T = 0.58 \pm 0.02$ and $\Phi_2^T = 0.96 \pm 0.05$ for PCA. For each of the esters one of the transition-state fractionation factors is essentially unity. Therefore, both nonlinear-least-squares fitting to a quadratic function and polynomial regression analysis support a linear dependence of reaction velocity on *n* for the studied reactions.

β-Deuterium Secondary Isotope Effects. β-D effects were determined by measuring initial velocities at $[S]_o \sim 7K$ and are listed in Table III. Isotope effects in the table are calculated for each adjacent pair of isotopic substrate runs. Two experiments under slightly different conditions give the same mean β-D effect within experimental error. The average of the two experiments is $0.96_0 \pm 0.01_7$. β-D effects for V/K were measured at $[ONPA]_o \ll K$ by fitting time course data to eq 2, as described in the Experimental Section. The mean for 22 determinations gives $^{D3}(V/K) = 1.00_2 \pm 0.02_6$.

Temperature Dependence of ONPA Hydrolysis. Initial velocities for AChE-catalyzed ONPA hydrolysis were measured at various temperatures in the range 11–38.2 °C. The Eyring plot[20] constructed from these data is nonlinear (Figure 3). The K value is slightly temperature sensitive over the studied range: K = 0.24 ± 0.04 mM at 14 °C, K = 0.28 ± 0.02 mM at 25 °C, and K = 0.38 ± 0.05 mM at 38 °C. $[ONPA]_o$ = 2.00 mM, so that initial velocities were measured at 89%, 88%, and 84% substrate saturation at the respective temperatures. Therefore, the nonlinearity of the Eyring plot cannot be a result of temperature-dependent changes in fractional saturation of the enzyme.[21] Another potential source of the nonlinearity of the plot is that the stability of AChE decreases as the temperature increases. This source is ruled out because the Eyring plot for V of AChE-catalyzed hydrolysis of *p*-methoxyphenyl formate is linear.[22] The nonlinearity of the Eyring plot could signal that two (or more) elementary steps contribute prominently to rate determination. In this case k_{cat} (and hence V) depends on the rate constants of both steps

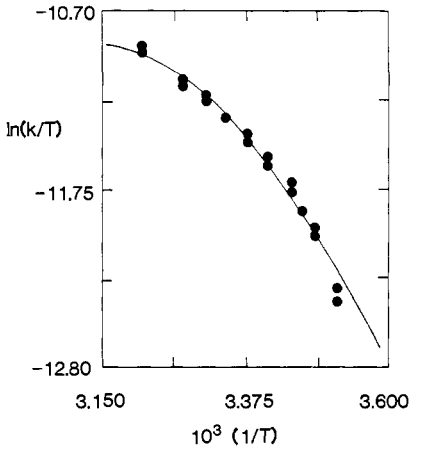

Figure 3. Eyring plot for initial velocities of AChE-catalyzed hydrolysis of ONPA. Reactions were conducted at various temperatures in 1.00 mL of 0.1 M sodium phosphate buffer, pH 7.30, that contained 0.1 N NaCl, 0.64 nM AChE ($[ONPA]_o$ = 2.00 mM), and 2% CH_3CN (v/v).

Scheme II

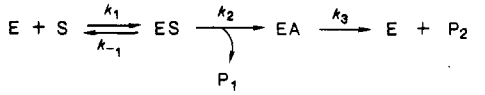

$$V^{-1} = (k_2[E]_T)^{-1} + (k_3[E]_T)^{-1} \quad (6)$$

The rate constants k_2 and k_3 are those for acetylation and deacetylation, respectively. The reasons for these assignments are given in the Discussion section. The Eyring equation derived from eq 6 is expressed as eq 7, where A and B correspond to k_2 and

$$\ln \frac{V}{T} = -\ln (Ae^{B/T} + Ce^{D/T}) \quad (7)$$

equal $e^{-\Delta S^{\ddagger}_2/R}\hbar/(k_B[E]_T)$ and $\Delta H_2^{\ddagger}/R$, respectively; C and D correspond to k_3 and have analogous meanings. The constants h, k_B, and R are Planck's constant, Boltzmann's constant, and the gas constant, respectively. The nonlinear line of Figure 3 resulted from least-squares fitting of the data to eq 7; the activation parameters determined from the fit are $\Delta H_2^{\ddagger}$ = 21.0 ± 0.4 kcal/mol, $\Delta S_2^{\ddagger}$ = 42 ± 1 eu, $\Delta H_3^{\ddagger}$ = 2.7 ± 0.3 kcal/mol, and $\Delta S_3^{\ddagger}$ = −21 ± 1 eu. Our least-squares estimate for $\Delta H_3^{\ddagger}$ compares well with the $\Delta H^{\ddagger}$ of 0–1.5 kcal/mol estimated by Wilson and Cabib[23] for the deacetylation stage of AChE-catalyzed hydrolysis of acetylcholine and dimethylaminoethyl acetate. The temperature at which $k_2 = k_3$ was calculated from the activation parameters is 289 ± 15 K. The solvent isotope effects for AChE-catalyzed hydrolysis of ONPA were determined at the extremes and in the middle of the Eyring plot and are temperature invariant: $^{D_2O}V_i$ = 1.91 ± 0.07, 1.90 ± 0.08, and 1.89 ± 0.06 at 10, 25, and 35 °C, respectively. The Eyring plot for V of AChE-catalyzed hy-

(19) Swain, C. G.; Kuhn, D. A.; Schowen, R. L. *J. Am. Chem. Soc.* **1965**, *87*, pp 1553–1561.
(20) Glasstone, S.; Laidler, K. J.; Eyring, H. *The Theory of Rate Processes*; McGraw-Hill: New York, 1941.
(21) Though the fractional substrate saturation of AChE does not change appreciably with temperature, the distribution of enzyme among stable bound states (i.e., ES and EA) may change. This situation arises if the acylation and deacylation rate constants (k_2 and k_3, respectively) have different temperature sensitivities. Equations 6 and 7 are based on such a model.
(22) Acheson, S. A.; Barlow, P. N.; Lee, G.; Swanson, M. L.; Quinn, D. M., following paper in this issue.
(23) Wilson, I. B.; Cabib, E. *J. Am. Chem. Soc.* **1956**, *78*, 202–207.

drolysis of PCA is also nonlinear downward (data not shown).

Discussion

The acylenzyme mechanism of AChE catalysis[2,3] and serine protease catalysis[5,6] is outlined in Scheme II, where EA is the acylenzyme intermediate, ES is the Michaelis complex, and P_1 and P_2 are the alcohol and acid products, respectively; a steady-state derivation of the corresponding phenomenological kinetic parameters gives eq 8–10. In eq 9 $K_s = (k_2 + k_{-1})/k_1$. Equation

$$V = \frac{k_2k_3}{k_2 + k_3}[E]_T \tag{8}$$

$$K = \frac{K_sk_3}{k_2 + k_3} \tag{9}$$

$$V/K = (k_2/K_s)[E]_T \tag{10}$$

8 shows that V depends on the rate constants for acylation (k_2) and for deacylation (k_3). For acyl-similar substrates, k_3 must be identical. That k_{cat}'s for each pair of acyl-similar substrates for AChE are of comparable magnitude (cf. Table I) indicates that deacylation is probably contributing to rate determination. Partial rate determination by deacylation is supported by the observation that V is linearly activated by increasing MeOH concentrations for AChE-catalyzed hydrolyses of ONPA and PCA.[24] However, k_3 cancels out of V/K regardless of the relative values of k_2 and k_3, so that V/K always monitors acylation.

Solvent isotope effects of Table I for V/K of AChE-catalyzed hydrolysis of phenyl esters are near unity, which indicates that chemical catalytic events that involve proton transfer are not contributing significantly to acylation rate determination for V/K. The solvent isotope effects for V/K of PA hydrolysis are 1.16 and 1.33, which compare favorably with $^{D_2O}(V/K)$ = 1.23 and 1.46 reported by Rosenberry.[4] He attributes the small solvent isotope effects for acetate ester substrates to prominent rate determination by an induced-fit conformation change that precedes chemical catalysis during the acylation stage of the AChE mechanism.[3,4] The pattern of small solvent isotope effects for acylation also holds for much less reactive anilide substrates of AChE.[22,25] For these substrates Acheson et al.[22] and Quinn and Swanson[25] showed that acylation is rate limited by a virtual transition state that consists of the transition state of a solvent isotope-sensitive and pH-sensitive microscopic step (30–40% rate determining) and the transition state of a microscopic step that is insensitive to pH and solvent isotope (60–70% rate determining). The former is likely the transition state of a chemical step, while the latter is likely the transition state of a physical event, such as conformation change or product release. The solvent isotope effects for V/K reported herein are also consistent with prominent (perhaps exclusive) acylation rate determination by a physical step(s). This model for acylation reaction dynamics and transition-state structure is supported by measurement of secondary isotope effects for ONPA hydrolysis. The lack of a β-D effect for V/K (i.e., $^{D3}(V/K)$ = 1.002) indicates that nucleophilic interaction between the active site serine and the carbonyl carbon of substrate is not an important structural feature of the acylation transition state.

The picture which emerges for V is very different than that for V/K. Solvent isotope effects for V of 1.6–2.26 indicate that proton transfer is an element of transition-state structure of microscopic steps monitored by V. The pL–rate profiles of Figure 1 show that the velocity of AChE catalysis depends on the basic form of an amino acid side chain that has a pK_a of 6.31 ± 0.03. This value is similar to the pK_a's of 6.5 and 6.56 reported by Rosenberry[4] for k_{cat} of AChE-catalyzed hydrolysis of acetylcholine and PA. As does Rosenberry, we interpret the pK_a in terms of general acid–base catalysis by an active site histidine imidazole side chain. The pK_a shifts 0.50 ± 0.06 pH unit when the reaction is monitored in D_2O, which is the solvent isotopic shift of pK_a that is expected for a weak organic acid.[16,17] This isotopic shift is the same within experimental error as that for the pK_a of imidazole (6.97 in H_2O, 7.46 in D_2O).[26]

The serine proteases display a great deal of transition-state structural plasticity as the substrate structure is varied.[7-11,27,28] For minimal substrates such as amino acid esters and amides and p-nitrophenyl acetate, proton inventories show that the serine proteases behave as one-proton catalysts. However, the serine proteases behave as two-proton catalysts (charge-relay catalysts) for reactions of peptide substrates that can interact with the enzymes' extended active sites. Therefore, as the interaction of enzyme and substrate in the transition state approaches that of the natural substrate (for which serine protease catalytic power has evolved), the full complement of transition state-proton transfers are expressed. One then might wonder whether AChE, whose mechanism is similar to that of the serine proteases, also behaves as a multiproton catalyst. Proton inventory experiments for V_i of AChE-catalyzed hydrolysis of ONPA and PCA at substrate concentrations near saturation give linear plots. These results are consistent with stabilization of AChE transition states by simple general acid–base catalysis. One-proton catalysis does not necessarily mean that the AChE active site does not consist of the triad of amino acids (serine, histidine, and aspartate) of the serine proteases. However, it is apparent that, even for the physiological deacetylation reaction, the coupled transfer of protons among the constituents of a putative active-site triad is not a feature of AChE catalysis.

The temperature dependence for $V_i \sim V$ of AChE-catalyzed hydrolysis of ONPA gives an Eyring plot that is nonlinear downward (cf. Figure 3). However, the solvent isotope effects measured at 10, 25, and 35 °C do not vary (cf. Results section). Should the source of the nonlinearity of the Eyring plot be a change in contribution to rate determination of serial microscopic steps, the individual steps must give the same isotope effect. Wilson and Cabib[23] described similar nonlinear temperature dependences for AChE-catalyzed hydrolysis of acetylcholine and dimethylaminoethyl acetate, which they interpret in terms of partial rate determination by both acylation (k_2) and deacylation (k_3). The step that has the lower $\Delta H^{\ddagger}$, and which therefore dominates the rate at high temperature, they assign to deacetylation; acetylation, which has the higher $\Delta H^{\ddagger}$, dominates the rate at low temperature. Froede and Wilson[29] recently trapped the acetylenzyme formed during AChE-catalyzed hydrolysis of acetylcholine. They found that 68% of the enzyme is in the acetylenzyme form, which they interpret as indicating that deacetylation and acetylation contribute 68% and 32%, respectively, to rate determination.

The simplest model that can accommodate the observations discussed in the last paragraph and the linear proton inventory for ONPA contains the following features. (a) The phenomenological transition state monitored by V is a virtual transition state that is a weighted average of acetylation and deacetylation contributions, wherein the weighting factors are fractions of rate determination by the individual steps. For ONPA, the weighting factors are estimated by using data in Table I and in the literature. Rosenberry[4] showed that k_{cat}'s for *Electrophorus electricus* AChE-catalyzed hydrolyses of PA and acetylcholine differed by only 7%. Similarly, Krupka[30] found that the k_{cat}'s for bovine erythrocyte AChE-catalyzed hydrolysis of these substrates differed by only 13%. Froede and Wilson[29] showed that acetylcholine turnover is 68% rate limited by deacetylation, and hence PA turnover must be similarly rate limited. However, since from the data of Table I one can calculate that V (and hence k_{cat}) for ONPA is 73% that for PA, ONPA hydrolysis is 50% rate limited

(24) Acheson, S. A.; Dedopoulou, D.; Quinn, D. M., unpublished results.
(25) Quinn, D. M.; Swanson, M. L. *J. Am. Chem. Soc.* **1984**, *106*, 1883–1884.
(26) Acheson, S. A.; Quinn, D. M., unpublished results. Our pK_a's agree well with those determined by: Li, N. C.; Tang, P.; Mathur, R. *J. Phys. Chem.* **1965**, *65*, 1074–1076.
(27) Pollock, E.; Hogg, J. L.; Schowen, R. L. *J. Am. Chem. Soc.* **1973**, *95*, 968.
(28) Quinn, D. M.; Elrod, J. P.; Ardis, R.; Friesen, P.; Schowen, R. L. *J. Am. Chem. Soc.* **1980**, *102*, 5358–5365.
(29) Froede, H. C.; Wilson, I. B. *J. Biol. Chem.* **1984**, *259*, 11010–11013.
(30) Krupka, R. M. *Biochemistry* **1966**, *5*, 1988–1998.

by deacetylation.[31] (b) The nonlinearity of the Eyring plot of Figure 3 for ONPA hydrolysis arises because both acylation and deacylation contribute to rate determination. The temperature independence of the solvent isotope effect obtains because at substrate saturation acylation and deacylation have the same intrinsic isotope effects. (c) The phenomenological proton inventory for ONPA hydrolysis (Figure 2A) is linear because the intrinsic proton inventories for acylation and deacylation are linear; i.e., the acylation and deacylation transition states are both stabilized by single-proton bridges.

The linear proton inventories of Figure 2 are mathematically described by an expression that is analogous to eq 6 and that contains linear dependences of the individual rate constants on the atom fraction of deuterium:

$$1/V_n = 1/\{k_2(1 - n + n\Phi_2^T)[E]_T\} + 1/\{k_3(1 - n + n\Phi_3^T)[E]_T\} \quad (11)$$

The rate constants are for the reaction in H_2O; Φ_2^T and Φ_3^T are the fractionation factors for the transferring protons of the acylation and deacylation stages of catalysis, respectively. Equation 11 is transformed to a more useful form by multiplying by V_o (cf. eq 8):

$$V_o/V_n = f_2/(1 - n + n\Phi_2^T) + f_3/(1 - n + n\Phi_3^T) \quad (12)$$

In eq 12 $f_2 = k_3/(k_2 + k_3)$ and $f_3 = k_2/(k_2 + k_3)$ are weighting factors that express the fractional contributions to the rate determination of acylation and deacylation, respectively. For ONPA the weighting factors were estimated in the preceding paragraph and are $f_2 = f_3 = 0.50$. The fractionation factors are both 0.53, which was calculated by least-squares analysis of the ONPA proton inventory data of Table II, as described in the Results section. With these stipulations in mind, eq 12 is transformed into eq 13. Equation 13 is just the best linear-least-squares fit

$$V_n = V_o\frac{1 - n + 0.53n}{0.50 + 0.50} \quad (13)$$

described in the Results section for the ONPA proton inventory. The proton inventory remains linear no matter what the individual weighting factors equal. Therefore, the model from which eq 12 springs also accounts for the linear proton inventory for PCA in Figure 2B, even though we do not have estimates of f_2 and f_3 at this time.

Two alternate models for the proton inventories follow. (a) Either acylation or deacylation (or both) involves concerted transfer of two protons. Consider, for example, a case in which the acylation transition state for ONPA hydrolysis is stabilized by two proton bridges that contribute equally to the solvent isotope effect. The requisite version of eq 12 for this case is:

$$V_o/V_n = \frac{0.50}{(1 - n + 0.73n)^2} + \frac{0.50}{1 - n + 0.53n} \quad (14)$$

The dotted line in Figure 2A is generated from this equation. Inclusion of a quadratic term for acylation degrades the fit of the ONPA proton inventory. If quadratic terms for both acylation and deacylation are used, the fit is even worse. (b) The intrinsic solvent isotope effects are not equal for the acylation and deacylation steps of the ONPA reaction. In the limiting case, one step has an isotope effect of 2.8 and the other no isotope effect,

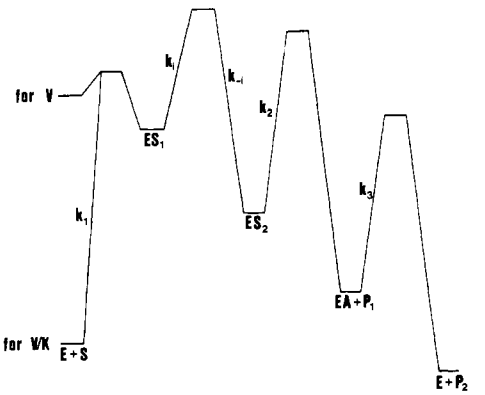

Figure 4. Free energy diagram for the AChE-catalyzed hydrolysis of ONPA. The steps denoted by the rate constants k_2 and k_3 are chemical catalytic steps for acylation and deacylation,[35] respectively; k_i is the rate constant for an induced-fit enzyme isomerization.[3,4] The course of the reaction is shown as energetically downhill from the Michaelis complex (ES_1) to the induced-fit complex (ES_2) because the solvent isotope effect for V of 1.89 (cf. Table I) arises from comparable contributions from the k_2 and k_3 steps. If ES_1 were of lower energy than ES_2, the k_i step would figure prominently in rate determination for V and would suppress the contribution of the k_2 step to the solvent isotope effect. The course of the reaction is shown as energetically downhill from ES_2 to EA because the reaction is not subject to product inhibition by *o*-nitrophenol.

so that an even mix of rate determination by acylation and deacylation produces the observed effect of 1.9. However, this situation will produce a proton inventory that is strongly bowed upward, as Quinn and Swanson showed for the acylation step of AChE-catalyzed hydrolysis of *o*-nitrochloroacetanilide.[25] Our proton inventory cannot exclude a case in which the two steps have comparable solvent isotope effects, such as 1.6 and 2.2. However, the fact that the solvent isotope effect does not vary with temperature indicates that the solvent isotope effects for the two steps must be closer in magnitude than 1.6 and 2.2.[32]

The β-D effect (cf. Table III) for V allows one to elaborate additional features of the transition-state structure for AChE-catalyzed hydrolysis of ONPA. The observed effect is inverse by 1.4 ± 0.6% per D. The isotope effect expected for complete conversion of the sp^2 substrate carbonyl to sp^3 in the transition state is 4.8% per D.[33,34] Hence, the ONPA isotope effect indicates

(31) Label the maximal velocities of Table I for PA and ONPA as V and V', respectively. The equations for the maximal velocities are $V = k_2k_3[E]_T/(k_2 + k_3)$ and $V' = k_2'k_3[E]_T/(k_2' + k_3)$. The rate constant k_3 is the same in the two equations because PA and ONPA have the same acyl group. When one divides the two equations, one gets $V/V' = (k_2/(k_2 + k_3))/(k_2'/(k_2' + k_3))$. The rate constant ratios in the quotient on the right-hand side of this equation are the fractional rate determinations for deacetylation (f_3) for PA and ONPA, respectively. Therefore, the fraction of rate determination by deacetylation for ONPA can be calculated from the corresponding value for PA. It should be noted that the estimated fraction of deacetylation rate determination for ONPA can tolerate considerable uncertainty in the V/V' ratio. If, for example, V/V' is 0.6 or 0.85 rather than 0.73, f_3 is 0.41 or 0.58, respectively. In any case, prominent rate determination by both acetylation and deacetylation is indicated.

(32) The projected temperature dependence of the observed solvent isotope effects is calculated as follows. (a) Calculate the temperature dependence of the intrinsic isotope effects (i.e., 1.6 and 2.2) by using the following equations, which are derived from the Eyring equation:[20] $^{D_2O}k_2 = 1.6 = e^{\Delta\Delta G_2^*/RT}$ and $^{D_2O}k_3 = 2.2 = e^{\Delta\Delta G_3^*/RT}$. These equations are used to calculate $\Delta\Delta G_2^*$ and $\Delta\Delta G_3^*$ at 298.15 K (25 °C). (b) *Case 1*: The difference in isotopic free energies of activation for each rate constant arises from the difference in enthalpies of activation, so that the intrinsic solvent isotope effects are temperature dependent (1.64, 1.60, and 1.58 for k_2 at 10, 25, and 35 °C, respectively; 2.29, 2.20, and 2.14 for k_3 at the same temperatures). (c) *Case 2*: The differences in isotopic entropies of activation dominate the free energy differences, so that the intrinsic solvent isotope effects are temperature independent. (d) The activation parameters calculated in the Results section were used to calculate how the rate constants change with temperature and hence how the fractions of rate determination by acetylation and deacetylation change. Like Wilson and Cabib,[23] we assign predominant rate determination at low temperature to acetylation and at high temperature to deacetylation. The predicted values for the observed solvent isotope effects are 1.82, 1.90, and 1.95 at 10, 25, and 35 °C, respectively, for case 1. For case 2, the predicted values are 1.77, 1.90, and 1.99 at the respective temperatures. If the intrinsic isotope effects for k_2 and k_3 are switched, the temperature dependence of the predicted isotope effects is even greater. In both cases the predicted isotope effects vary to an extent that is greater than the experimental uncertainty of the isotope effects reported in the Results Section. Therefore, the temperature insensitivity of our measured solvent isotope effects rules out the possibility that the intrinsic solvent isotope effects are 1.60 and 2.20. However, our measured isotope effects cannot rule out the possibility that the intrinsic isotope effects are 1.70 and 2.10.

(33) Hogg, J. L.; Rodgers, J.; Kovach, I.; Schowen, R. L. *J. Am. Chem. Soc.* **1980**, *102*, 79–85.

(34) Kovach, I. M.; Hogg, J. L.; Raben, T.; Halbert, K.; Rodgers, J.; Schowen, R. L. *J. Am. Chem. Soc.* **1980**, *102*, 1991–1999.

(35) The rate constants k_2 and k_3 may each be composite rate constants that are comprised of contributions from two or more microscopic events (e.g., formation and breakdown of tetrahedral intermediates, proton transfers, etc.).

that there is 30 ± 10% sp^2 to sp^3 conversion of the substrate carbonyl in the transition state. There are two limiting possibilities for these β-D observations. (a) Both the acetylation and deacetylation transition states involve nucleophilic interaction between AChE and substrate that results in 30% conversion at the substrate carbonyl. For either acetylation or deacetylation the effect could arise from an early transition state for formation of a tetrahedral intermediate or from a late transition state for decomposition of a tetrahedral intermediate. (b) An intrinsic β-D effect of 2.8% per D for acetylation (or deacetylation) is partially masked by a deacetylation (or acetylation) transition state that is 50% rate determining and that gives no β-D effect. We cannot decide between these possible accountings of the β-D effect at this time. Nonetheless, we can say that in the acetylation or deacetylation transition state (or both) proton transfer and nucleophilic AChE–substrate interaction are occurring simultaneously.

The virtual ONPA transition state holds added significance for the reaction dynamics of the acylation stage of AChE catalysis. As discussed above, the virtual transition state is comprised of acetylation and deacetylation contributors that each are manifested by sizable solvent isotope effects. However, the solvent isotope effect for V/K is scarcely different from unity (cf. Table I). V/K always monitors the rate-determining step through the first irreversible event of the catalytic reaction. In an acylenzyme mechanism the first irreversible step must be coincident with or precede the release of P_1. Therefore, the commitment to chemical catalysis in the acetylation stage of AChE-catalyzed hydrolysis of ONPA must be ~10 (see below), which would reduce an intrinsic solvent isotope effect of 1.9 to that observed for V/K in Table I. This large commitment requires either that binding of ONPA or some isotope-insensitive step that succeeds the Michaelis complex but precedes chemical catalysis is limiting the acetylation rate. Acheson et al.[22] and Quinn and Swanson[25] calculated commitments of 1.4–2.5 for the acylation stage of AChE-catalyzed hydrolysis of various anilides that have k_{cat}/K's that are 2–4 orders of magnitude lower than that of ONPA. It seems unlikely that binding would be rate determining for the much less reactive anilides. Therefore, Rosenberry's induced-fit model[3,4] may be a general theme for the reaction dynamics of the acylation stage of AChE catalysis. Figure 4 contains a qualitative free energy diagram for AChE-catalyzed hydrolysis of ONPA that is consistent with these observations. The free energy diagram contains a step in addition to those shown in Scheme II. This extra step, which occurs during acylation, interconverts ES_1 and ES_2 and is probably an enzyme isomerization.[3,4,22,25] The chemical steps of acylation and deacylation, which have transition states that are stabilized by single-proton bridges,[36] have rate constants k_2 and k_3, respectively. When $[S]_o \gg K$ (i.e., V kinetics), the enzyme is saturated as ES_2 and EA and k_2 and k_3 contribute approximately equally to rate determination. However, when $[S]_o \ll K$ (i.e., V/K kinetics), the reactant state is E + S and k_1 is the rate-determining step. Hence, the solvent isotope effect for k_2 is masked by the large commitment to proton-transfer catalysis,[37] k_2/k_{-1}.

In summary, V for AChE-catalyzed hydrolysis of aryl esters is rate limited by a virtual transition state that is comprised of contributions from the chemical transition states for acylation and deacylation. V/K, which always monitors only acylation, is similarly rate limited by a virtual transition state. In contrast to the virtual transition state for V, that for V/K is dominated by a physical step that precedes chemical catalysis. The following two papers further explore transition-state structures, acylation dynamics, and thermodynamics for AChE catalysis.

Acknowledgment. This work was supported by NIH Grant NS21334. D.M.Q. is the recipient of a NIH Research Career Development Award (HL01583).

Registry No. AcOPh, 122-79-2; *o*-$AcOC_6H_4NO_2$, 610-69-5; $ClCH_2CO_2Ph$, 620-73-5; *p*-$ClCH_2CO_2C_6H_4OMe$, 36560-13-1; $ClCH_2C-O_2COCH_2Cl$, 541-88-8; PhOH, 108-95-2; acetylcholinesterase, 9000-81-1.

(36) Kovach et al. have recently shown that V for AChE-catalyzed hydrolysis of phenyl acetate is rate limited by a transition state that is stabilized by single-proton bridging: Kovach, I. M.; Larson, M.; Schowen, R. L. *J. Am. Chem. Soc.* **1986**, *108*, 3054–3056.

(37) Acheson et al.[22] show that the solvent isotope effect for V/K is given by an expression like $^{D_2O}V/K = (^{D_2O}k_2 + C)/(1 + C)$, where $C = k_2/k_{-1}$. Hence, if $^{D_2O}k_2 = 1.9$ and C is 10, $^{D_2O}V/K$ is 1.08, which agrees with the effect for ONPA that is given in Table I.